JOURNAL OF Materials CHEMISTRY

Synthesis and properties of novel donor-type metal–dithiolene complexes based on 5,6-dihydro-1,4-dioxine-2,3-dithiol (edo) ligand†

Eiji Watanabe,[a] Masahiro Fujiwara,[a] Jun-Ichi Yamaura[a] and Reizo Kato*[b]

[a]*The Institute for Solid State Physics, The University of Tokyo, Kashiwa-shi, Chiba 277-8581, Japan*
[b]*RIKEN (The Institute of Physical and Chemical Research), Hirosawa, Saitama 351-0198, Japan. E-mail: reizo@postman.riken.go.jp*

Received 6th March 2001, Accepted 2nd May 2001
First published as an Advance Article on the web 8th June 2001

A novel donor-type metal–dithiolene complex, Ni(edo)$_2$ [edo = 5,6-dihydro-1,4-dioxine-2,3-dithiolate], and its mixed-ligand derivatives were synthesized and characterized. Their improved solubility and donor abilities have been confirmed. They provide various types of radical cation salts which exhibit novel donor arrangements.

Metal–dithiolene complexes form very attractive categories of molecular metals and superconductors. They can have various oxidation states and can range from electron acceptors to donors. The first observation of metallic behavior in crystalline metal–dithiolene complexes was reported for $Li_{0.75}[Pt(mnt)_2]\cdot 2H_2O$ [mnt = maleonitriledithiolate; Scheme 1] by Underhill *et al.* in 1981.[1] The conduction pathway in molecular conductors based on metal–dithiolene complexes is *via* mixed metal(d)–ligand(π) orbitals where the S atoms play an important role. This is in contrast to the case of the partially oxidized conducting platinum complexes, including $K_2[Pt(CN)_4]Br_{0.3}\cdot 3H_2O$ (KCP), where a one-dimensional conduction band is formed by the metal d orbital and there is no contribution by the ligand to the conduction band. Another important character of the square-planar metal–dithiolene complex is that the metal d orbitals cannot mix into the HOMO (highest occupied molecular orbital) due to the symmetry while the metal d_{xz} orbital has the appropriate symmetry to mix into the LUMO (lowest unoccupied molecular orbital).[2] This leads to the small energy gap between HOMO and LUMO. Therefore, both the HOMO and LUMO can play an important role in the formation of the conduction band depending on the molecular arrangement.

Acceptor-type metal–dithiolene complexes M(dmit)$_2$ [dmit = 2-thioxo-1,3-dithiole-4,5-dithiolate, M = Ni, Pd, Pt, Au; Scheme 1] have provided various conducting radical anion salts which have been extensively studied.[3] Radical anion salts of Pd(dmit)$_2$ with a monovalent cation Z^+, Z[Pd(dmit)$_2$]$_2$, are unique two-band systems associated with the HOMO and LUMO bands.[4] In crystals of Z[Pd(dmit)$_2$]$_2$, a strong dimerization of the Pd(dmit)$_2$ units along the stack is observed. In the dimer, both the HOMO and LUMO generate bonding and anti-bonding orbitals separated by an energy gap. When the dimers are assembled into a conduction layer, a "HOMO–LUMO" band inversion occurs because the dimerization gap is large compared with the HOMO–LUMO gap (ΔE). The conduction band is the HOMO band which lies above the LUMO band.

The donor-type metal–dithiolene complexes, where the central C=C bond in the TTF-based organic donor is replaced by a transition metal, are also promising materials. For example, M(dddt)$_2$ [dddt = 5,6-dihydro-1,4-dithiine-2,3-dithiolate, M = Ni, Pd, Pt, Au; Scheme 1] complexes which correspond to the organic π-donor BEDT-TTF (ET) [bis(ethylenedithio)-tetrathiafulvalene; Scheme 1] are known to provide various conductors. For example, $[Ni(dddt)_2]_3(AuBr_2)_2$ is the first metallic radical cation salt of a metal–dithiolene complex which is stable down to at least 1.3 K.[5] The "HOMO–LUMO" band inversion can also be observed in the donor-type system. The "HOMO–LUMO" band inversion in the donor-type metal–dithiolene system results in the LUMO band as the conduction band. This is the opposite to what is observed in the acceptor system. One drawback with the conventional donor-type metal–dithiolene complexes with the dddt complex is that they are poorly soluble in the usual organic solvents, and hence the preparation of high quality radical cation salts is difficult. In order to improve the solubility and expand the materials chemistry of the donor-type metal–dithiolene complex, we have directed our attention to M(edo)$_2$ [edo = 5,6-dihydro-1,4-dioxine-2,3-dithiolate; Scheme 1] as an analog of the organic donor BEDO-TTF (BO) [bis(ethylenedioxo)tetrathiafulvalene; Scheme 1]. This donor molecule which is soluble in various organic solvents is known to provide superconducting radical cation salts.[6]

We should also emphasize that a large number of

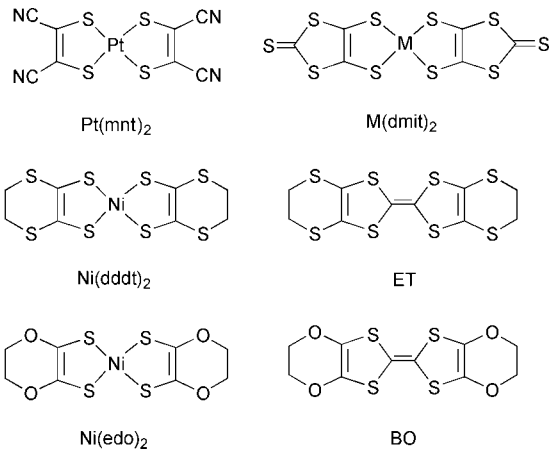

Scheme 1

†Electronic supplementary information (ESI) available: Conditions for crystal growth. See http://www.rsc.org/suppdata/jm/b1/b102000p/

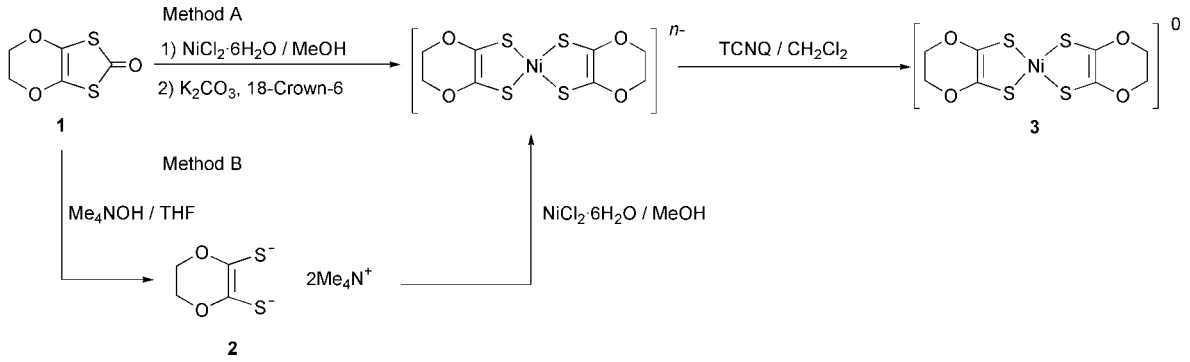

Scheme 2

"unsymmetrical" tetrachalcogenafulvalenes have been synthesized and have enriched the chemistry and physics of the molecular metals and superconductors.[7] In general, they show improved solubility compared with symmetrical species. These unsymmetrical organic donors can be synthesized by cross-coupled reactions of the corresponding units followed by liquid chromatography separation of the cross-coupled product from the self-coupled products. However, there was no systematic and general method for the synthesis of mixed-ligand (unsymmetrical) metal–dithiolene complexes. We have found that monoanionic mixed-ligand metal–dithiolene complexes can be easily obtained by ligand-exchange reactions between parent complexes followed by reversed phase chromatography separation,[8] and the mixed-ligand metal complexes obtained were classified as the acceptor system. A study of mixed-ligand species is also important in the donor-type metal–dithiolene complexes. It should be noted that the solubility of the target species is crucial to the chromatography separation and the edo ligand is expected to increase the solubility of the mixed-ligand species.

In this paper, we report on the synthesis and electrochemical properties of $Ni(edo)_2$ and its mixed-ligand derivatives, and structural and physical properties of their radical cation salts.

Results

Synthesis, electrochemistry, and crystal structure of $Ni(edo)_2$ and its mixed-ligand derivatives

Synthesis. We have failed to prepare the metal complex $Ni(edo)_2$ by the conventional procedure, that is, the ring opening of ketone (**1**)[4] with alkali [NaOMe or K_2CO_3/18-crown-6] followed by the addition of $NiCl_2$ in MeOH. This is because dianion **2** produced by the ring opening reaction rapidly decomposes in solution. We found that the addition of $NiCl_2$ *before* the ring opening of **1** in MeOH affords violet $[Ni(edo)_2]^{n-}$ (probably $n=2$) which can be oxidized to the deep blue neutral species **3** by TCNQ (Method A, Scheme 2). After this finding, we noticed that the dianion **2** can be isolated as a Me_4N^+ salt when the ketone **1** was treated with Me_4NOH in THF. Treatment of this Me_4N^+ salt with $NiCl_2$ followed by the TCNQ oxidation also gave neutral $Ni(edo)_2$ with an improved yield (Method B). Neutral $Ni(edo)_2$ is soluble in various organic solvents and easily purified by column chromatography (silica gel, CH_2Cl_2).

Mixed-ligand complexes were obtained by the ligand-exchange reaction between $Ni(edo)_2$ and the corresponding donor-type complexes $[Ni(L)_2]^0$ (L = dddt, ddds, ddt, pdt, dtm, where ddds = 5,6-dihydro-1,4-dithiine-2,3-diselenolate, ddt = 1,4-dithiine-2,3-dithiolate, pdt = 6,7-dihydro-5*H*-1,4-dithiepine-2,3-dithiolate, dtm = 1,2-bis(methylthio)ethylene-1,2-dithiolate) with a molar ratio of 1 : 1 (Scheme 3). In the case of the monoanionic complexes, acetone was used as solvent.[8] In the ligand-exchange reaction between the neutral donor-type complexes, refluxing 1,2-dichloroethane is more effective as solvent because the solubility of $[Ni(L)_2]$ is very low. After the reaction, the remaining $[Ni(L)_2]$ complex was easily separated by filtration. The column chromatography (silica gel, CS_2–CH_2Cl_2) of the reaction mixture afforded [Ni(edo)(L)] with moderate yields and recovered $Ni(edo)_2$. These procedures can be repeated by the use of recovered parent complexes to improve the practical yields.

We obtained another two mixed-ligand complexes [Ni(edo)(L)] (L = dmit and mnt) accidentally. They were formed by the ligand-exchange reaction which occurred in the electrolysis of solutions containing $Ni(edo)_2$ and $Bu^n{}_4N[Ni(L)_2]$. In contrast to other [Ni(edo)(L)] complexes, they are sparingly soluble in organic solvents.

Electrochemistry. Table 1 shows electrochemical data for $Ni(edo)_2$, mixed-ligand complexes and the parent complexes for comparison. $Ni(edo)_2$ shows two pairs of reversible redox waves at −1.55 and −0.86 V (*vs.* $Ag/AgNO_3$) corresponding to the $[Ni(edo)_2]^{2-}/[Ni(edo)_2]^-$ and $[Ni(edo)_2]^-/[Ni(edo)_2]^0$ couples, respectively. These potentials are negatively shifted from those of $Bu^n{}_4N[Ni(dddt)_2]$, which indicates that $Ni(edo)_2$ has a stronger donor ability than $Ni(dddt)_2$. The same relationship is observed between ET and BO.[9] Moreover, $Ni(edo)_2$ shows an irreversible oxidation wave at 0.11 V which is 0.17 V lower than that of $Bu^n{}_4N[Ni(dddt)_2]$.

Electrochemical data of the mixed-ligand complexes suggest that each redox potential shows the mean value of those for the corresponding parent species except for E_3 of Ni(ddds)(edo).

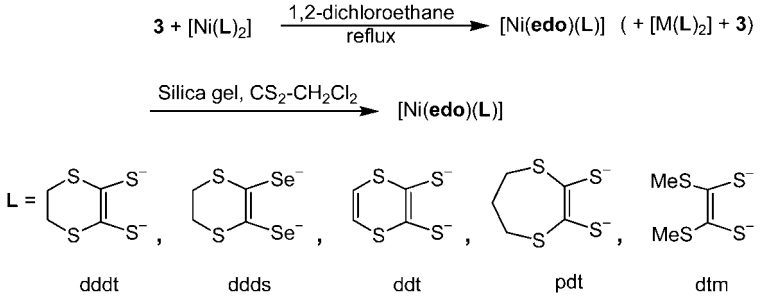

Scheme 3

Table 1 Cyclic voltammetric data

Metal complexes	E_1/V $(-2/-1)^a$	E_2/V $(-1/0)^a$	E_3/V $(0/+1)^b$
$Ni(edo)_2$ **3**	−1.55	−0.86	0.11
Ni(dddt)(edo)	−1.46	−0.73	0.19
Ni(ddds)(edo)	−1.46	−0.72	0.15
Ni(ddt)(edo)	−1.42	−0.68	0.10
Ni(edo)(pdt)	−1.53	−0.75	0.19
Ni(dtm)(edo)	−1.53	−0.82	0.03
Ni(dmit)(edo)	−1.29	−0.56	0.29
Ni(edo)(mnt)	−1.23	−0.43	
$Ni(dddt)_2$	−1.34	−0.59	-0.28
$Ni(ddds)_2$	−1.27	−0.51	-0.08
$Ni(ddt)_2$	−1.21	−0.49	-0.21
$Ni(pdt)_2$	−1.39	−0.52	0.26
$Ni(dtm)_2$	−1.39	−0.72	0.05
$Ni(dmit)_2$	−0.86	−0.30	
$Ni(mnt)_2$	−0.50	0.41	

[a]Reversible. [b]Irreversible wave.

Such a tendency is also observed in unsymmetrical organic donor molecules.[10] This means that electrochemical properties of the mixed-ligand metal–dithiolene complexes can be tuned by the ligand combination.

Crystal structure. Single crystals of neutral $Ni(edo)_2$ suitable for X-ray structural analysis were obtained by the slow recrystallization from the CH_2Cl_2–Pr^iOH solution. The unit cell contains two $Ni(edo)_2$ molecules, each of which is repeated uniformly along the *c* axis (Fig. 1). Two halves of the $Ni(edo)_2$ units are crystallographically independent. Each Ni atom in these two units lies on the inversion center. These independent molecules are similar to each other in bond lengths and conformation. Both $Ni(edo)_2$ molecules are planar except for the terminal ethylene groups, and this is also the case of the neutral $Ni(dddt)_2$ molecule.[11] It should be noted that the corresponding organic donors ET and BO are non-planar in the neutral state. The averaged bond lengths of Ni–S, S–C and C=C are 2.15, 1.68 and 1.41 Å, respectively. The Ni–S bond length in $Ni(edo)_2$ is slightly longer than that in $Ni(dddt)_2$ (2.12 Å).

Single crystals of neutral [Ni(dmit)(edo)] were grown by the electrolysis of a solution containing $Ni(edo)_2$ and $Bu^n{}_4N$[Ni(dmit)$_2$] in 1,2-dichloroethane. Fig. 2 shows the crystal structure of Ni(dmit)(edo). The unit cell contains four

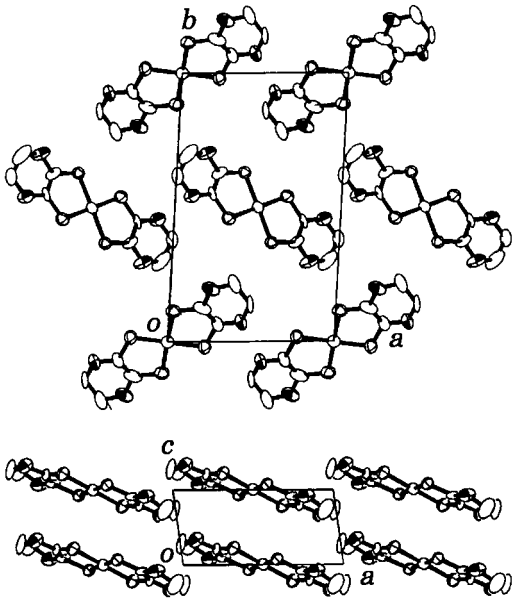

Fig. 1 Crystal structure of $Ni(edo)_2$ **3**.

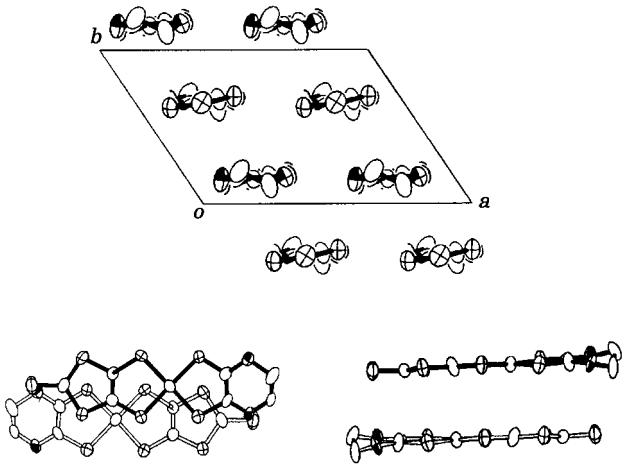

Fig. 2 Crystal structure of Ni(dmit)(edo).

[Ni(dmit)(edo)] molecules, one of which is crystallographically independent. The [Ni(dmit)(edo)] unit is almost planar and repeated in a head-to-tail fashion along the *c* axis. The averaged bond lengths of Ni–S, S–C and C=C are 2.15, 1.70 and 1.39 Å, respectively. Single crystals of [Ni(edo)(mnt)] were also obtained by a similar procedure from a solution containing $Ni(edo)_2$ and $Bu^n{}_4N[Ni(mnt)_2]$ in chlorobenzene. As shown in Fig. 3, the unit cell contains four [Ni(edo)(mnt)] molecules, one of which is crystallographically independent. The [Ni(edo)(mnt)] molecules are arranged alternately along the *c* axis. The averaged bond lengths of Ni–S, S–C and C=C are 2.15, 1.69 and 1.39 Å, respectively.

Structural and physical properties of radical cation salts

The galvanostatic oxidation of the donor-type metal–dithiolene complexes in the presence of the corresponding counter anion (X^-) provided radical cation salts, such as $[Ni(edo)_2]_3(X)_2$ with $X=ClO_4$, PF_6, SbF_6, $[Ni(edo)_2]_2(X)$ with $X=FeCl_4$, $GaCl_4$, $FeBr_4$, AsF_6, $[Ni(dddt)(edo)]_3(X)_2$ with $X=PF_6$, AsF_6, SbF_6, $FeCl_4$, $FeBr_4$, $[Ni(ddds)(edo)]_3(PF_6)_2$, $[Ni(ddds)(edo)]_2(FeCl_4)$, $[Ni(ddt)(edo)]_2(X)$ with $X=BF_4$, PF_6, $FeCl_4$, $GaCl_4$, $[Ni(edo)(pdt)]_3(PF_6)_2$, $[Ni(edo)(pdt)](X)$ with $X=ClO_4$, $FeCl_4$, $GaCl_4$, and $[Ni(dtm)(edo)]_2(X)$ with $X=ClO_4$, $FeCl_4$. Their stoichiometry could be determined by EPMA (electron probe microanalysis). Further characterization is provided by the crystal structure determinations and conductivity measurements for six salts.

$[Ni(edo)_2]_3(PF_6)_2$. The unit cell contains six $Ni(edo)_2$ molecules (Fig. 4). One and a half $Ni(edo)_2$ units are crystallographically independent (molecules **A** and **B** in Fig. 4). The

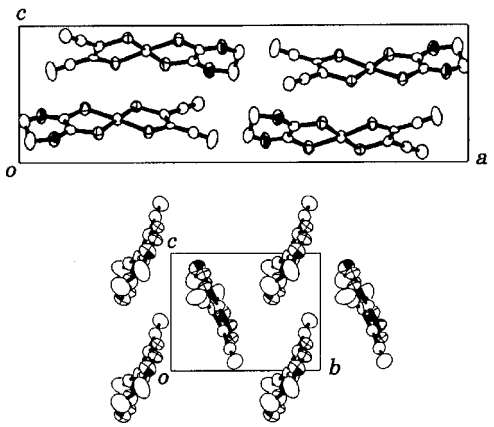

Fig. 3 Crystal structure of Ni(edo)(mnt).

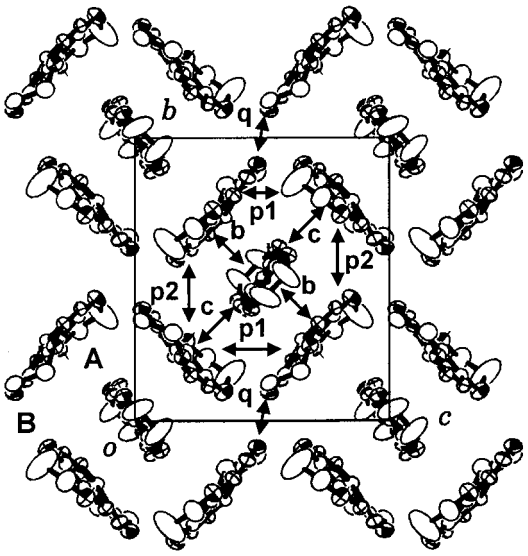

Fig. 4 Donor arrangement in $[Ni(edo)_2]_3(PF_6)_2$ viewed along the molecular long axis.

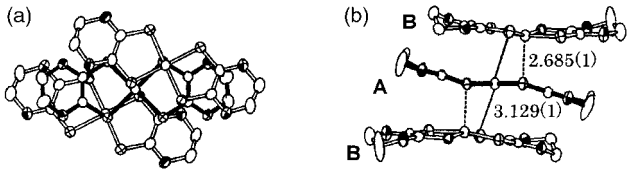

Fig. 5 Trimer in $[Ni(edo)_2]_3(PF_6)_2$.(a) top view, (b) side view.

Ni atom in the molecule **A** is located on the inversion center. The $Ni(edo)_2$ molecules form trimers which are packed almost perpendicularly to each other. This structural feature reminds us of the κ-type arrangement, which is frequently observed in the high-T_c ET-based superconductors.[12] In the κ-type ET salts, the donor molecules form face-to-face "dimers". The dimer has the thickness (=the inter-planar spacing) almost equal to the width (=the length of the short molecular axis), which is suitable for the orthogonal packing. Therefore, it appears difficult for trimers to form orthogonal packing. Fig. 5 shows the side and top views of the trimer. The central molecule (**A**) spans two terminal molecules (**B**) which exhibit a transverse slip. This is a kind of "spanning overlap" which was first found in the two-dimensional metal α-$Et_2Me_2N[Ni(dmit)_2]_2$.[13] This novel overlapping mode, which enlarges the width of the trimer to fit the thickness of the adjacent trimer, is the trick for the formation of the trimer-based κ-type packing.

The molecule **A** has a chair-conformation, while the molecule **B** has a boat-conformation. This indicates that the overlapping edo ligands repel each other. The averaged bond lengths for Ni–S, S–C and C=C in the dithiolene skeleton of the molecule **A** are 2.19, 1.70 and 1.39 Å, respectively, and those for the molecule **B** are 2.17, 1.68 and 1.42 Å, respectively. These differences in the conformation and the bond lengths suggest disproportionation of the formal charge between the molecules **A** and **B**. The present data, however, are not enough for more detailed analysis. The inter-planar distance between molecules **A** and **B** is 3.013 Å. The Ni atom in the molecule **A** exhibits an elongated octahedral coordination and the Ni atom in the molecule **B** is penta-coordinated (Fig. 5). Intermolecular metal–ligand contacts Ni(**A**)···S(**B**) and Ni(**B**)···S(**A**) are 3.129(1) and 2.685(1) Å, respectively. Similar coordination geometries are also observed in $Ni(dddt)_2$ salts.[14] In the trimer, S···S distances (3.313(2) Å) shorter than the van der Waals distance are observed, and there are no short inter-trimer O···O, S···S and O···S distances. The PF_6^- anions lie between the donor layers and are located far from the molecules **A** and close to the molecules **B**.

Table 2 Calculated overlap integrals (S) between frontier orbitals ($\times 10^3$) for $[Ni(edo)_2]_3(PF_6)_2$ (See Fig. 4)

S	HOMO–HOMO	LUMO–LUMO	HOMO–LUMO
b	−53.27	±8.58	±46.28, 6.09
c	−1.35	±3.15	±7.69, −1.13
p1	−5.82	0.98	−3.01, 5.83
p2	−0.57	0.61	−0.65, 0.49
q	0.38	0.62	−0.48,

The overlap integrals for the frontier orbitals (HOMO and LUMO) are listed in Table 2. Calculations were based on the extended Hückel approximation. Large intra-trimer interactions (|b| in Fig. 4) indicate strong trimerization. We cannot neglect intra-trimer HOMO···LUMO interactions in the present case. In $Z[Pd(dmit)_2]_2$, the intra-dimer HOMO···LUMO interaction is negligible. This is because two $Pd(dmit)_2$ units in the dimer adopt an eclipsed configuration and the symmetry of the HOMO is different from that of the LUMO. On the other hand, the spanning configuration in the trimer in $[Ni(edo)_2]_3(PF_6)_2$ is the one which provides the large HOMO···LUMO interactions. In the trimer, each HOMO and LUMO generates bonding, anti-bonding, and non-bonding orbitals. The tight-binding band calculation indicates that the HOMO–LUMO band inversion does not occur without the intra-trimer HOMO···LUMO interactions. Although this calculation was performed with an assumption that all the $Ni(edo)_2$ cations have the same formal charge ($+\frac{2}{3}$), the result is suggestive of a mechanism of the HOMO–LUMO band inversion. Introduction of the intra-trimer HOMO···LUMO interactions causes the HOMO–LUMO band inversion as shown in Fig. 6. Each band has a very narrow band width. The lower four bands in Fig. 6 are fully occupied and thus this calculation predicts that the present system is a semiconductor with an energy gap. Indeed, $[Ni(edo)_2]_3(PF_6)_2$ shows semiconductive behavior in its electrical resistivity ($\rho_{rt}=1.1\times10^4\ \Omega$ cm, $E_a=0.2$ eV).

$[Ni(edo)_2]_2FeCl_4$. The unique trimer structure of the $Ni(edo)_2$ unit is also observed in the 2:1 $FeCl_4$ salt. This salt is an insulator. Fig. 7 shows the donor arrangement in the *ac* plane. The unit cell contains four $Ni(edo)_2$ units (**A**, **B**, **B′**, **C**). The molecules **A** and **C** lie on the inversion centers. The molecules **B** and **B′** are related by the inversion symmetry. Molecules **A**, **B**, and **B′** form a trimer similar to that in

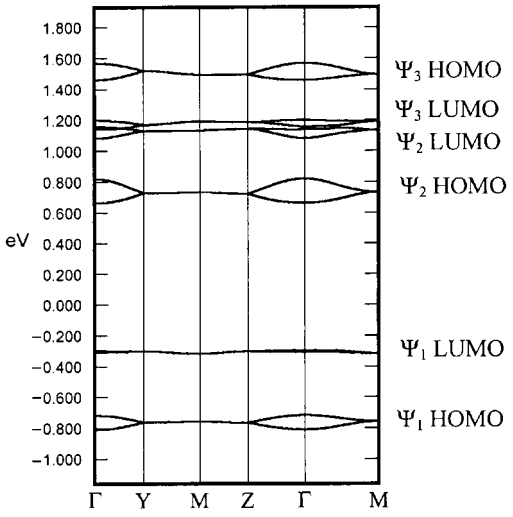

Fig. 6 Calculated band structure of $[Ni(edo)_2]_3(PF_6)_2$. The points in the reciprocal space are named Γ(0,0,0), Y(0,π/*b*,0), Z(0,0,π/*c*), M(0, π/*b*, π/*c*), respectively.

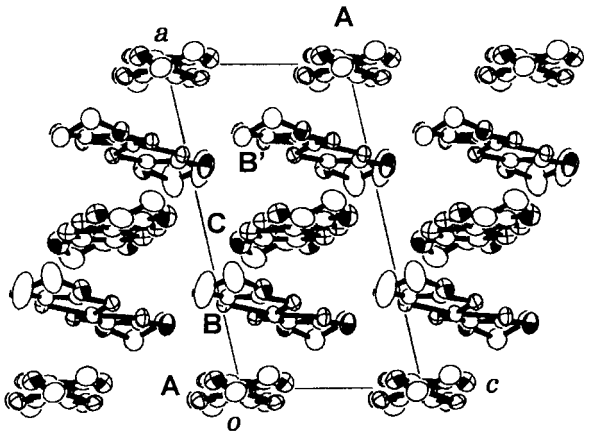

Fig. 7 Donor arrangement in $[Ni(edo)_2]_2FeCl_4$.

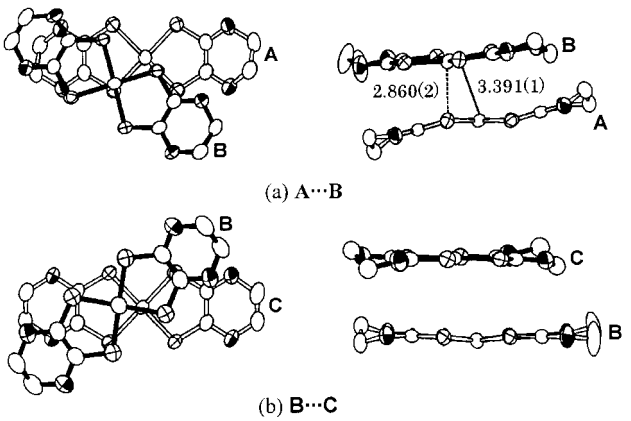

Fig. 8 Modes of overlap in $[Ni(edo)_2]_2FeCl_4$.

$[Ni(edo)_2]_3(PF_6)_2$. The inter-planar distance between molecules **A** and **B**(**B**′) is 3.092 Å, while the one between molecules **B**(**B**′) and **C** is 3.546 Å. Between molecules **A** and **B**(**B**′), short inter-molecular metal–ligand contacts Ni(**A**)···S(**B**) (3.391(1) Å) and Ni(**B**)···S(**A**) (2.860(2) Å) are observed, while there is no short inter-molecular metal–ligand contact between molecules **B** and **C**. The mode of overlap of the trimers is shown in Fig. 8. In contrast to the molecules **A** and **B**, the molecule **C** is fairly planar. The averaged bond lengths for Ni–S, S–C and C=C in the dithiolene skeleton are 2.18, 1.69 and 1.39 Å in the molecule **A**, 2.16, 1.67 and 1.42 Å in the molecule **B**, and 2.15, 1.68 and 1.39 Å in the molecular **C** . Considering that 1) the trimer in $[Ni(edo)_2]_3(PF_6)_2$ has the formal charge of +2 and 2) the neutral $Ni(edo)_2$ molecule is planar, we anticipate that the charge separation is ·····$[trimer]^{2+}[Ni(edo)_2]^0[trimer]^{2+}$-$[Ni(edo)_2]^0$····· along the $a+c$ direction. The $FeCl_4^-$ anions lie between the donor layers.

The tight-binding band calculation with an assumption that all the $Ni(edo)_2$ cations have the same formal charge ($+\frac{1}{2}$) is suggestive of the insulating nature of this salt. Since the calculation including both HOMO and LUMO indicated that the HOMO–LUMO band inversion does not occur in this system, we will discuss only the HOMO band. Calculated overlap integrals between the HOMOs are listed in Table 3. The major interactions are observed along the $a+c$ direction (a1 and a2). This system is one-dimensional and the repeat unit along the chain contains four donor molecules. Therefore, the HOMO band has four branches, each of which is separated by an energy gap. Fig. 9 shows a calculated band structure with the $\frac{3}{4}$-filling, which explains the insulating behavior of this salt.

$[Ni(edo)_2]_2FeBr_4$. The crystal structure of this insulating salt is closely related to that of the $FeCl_4$ salt. The unit cell contains

Table 3 Calculated overlap integrals (S) between HOMO's ($\times 10^3$) for $[Ni(edo)_2]_2FeCl_4$

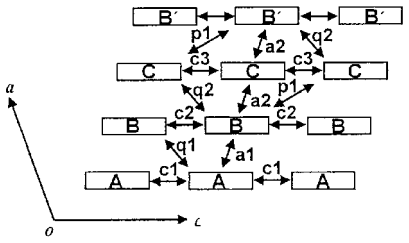

S	HOMO–HOMO
a1	−49.49
a2	−17.91
c1	0.24
c2	0.70
c3	0.20
p1	0.004
q1	−2.12
q2	−0.71

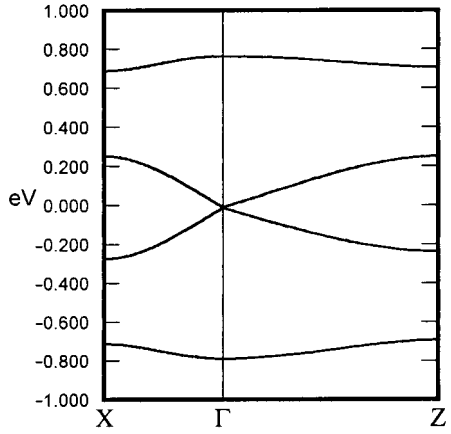

Fig. 9 Calculated band structure of $[Ni(edo)_2]_2FeCl_4$. The points in the reciprocal space are named Γ(0,0,0), X(π/a,0,0), Z(0,0,π/c), respectively.

sixteen $Ni(edo)_2$ units which form two (crystallographically equivalent) donor layers separated by the $FeBr_4$ anions. Within the donor layer, there are two types of donor columns (**1** and **2** in Fig. 10) along the c axis, while the donor layer in the $FeCl_4$

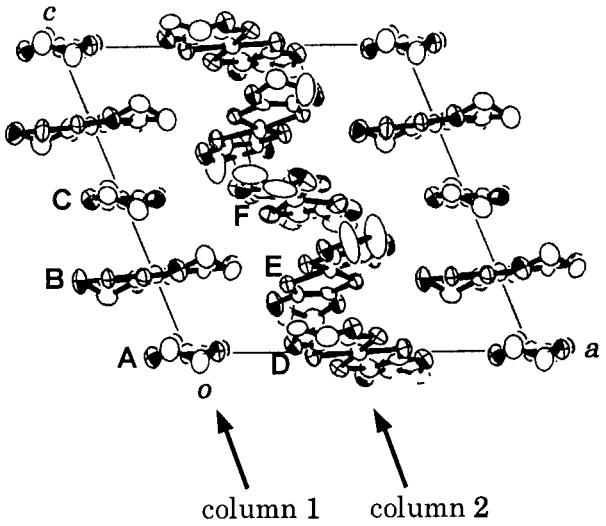

Fig. 10 Donor arrangement in $[Ni(edo)_2]_2FeBr_4$.

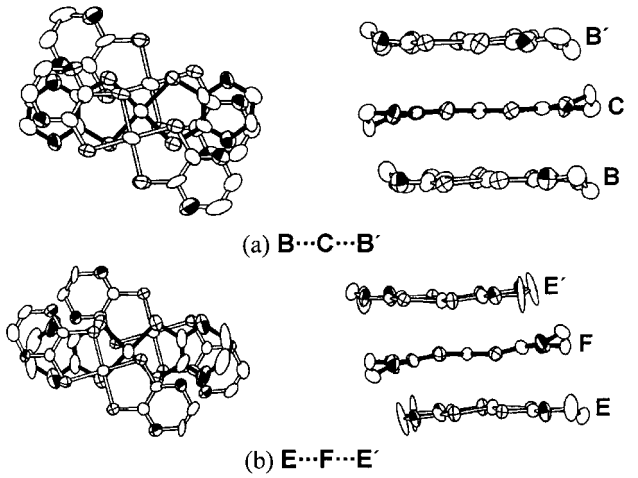

Fig. 11 Modes of overlap in $[Ni(edo)_2]_2FeBr_4$.

salt is formed by the repeat of one donor stack along the side-by-side direction (the *c* axis). The stack **1** contains molecules **A**, **B**, **C**, **B′** (molecules **B** and **B′** are related by the inversion symmetry) and the stack **2** contains molecules **D**, **E**, **F**, **E′** (molecules **E** and **E′** are related by the inversion symmetry). The molecules **A**, **C**, **D** and **F** lie on the inversion centers. In the stack **1**, inter-planar distances are 3.499 Å (between molecules **A** and **B**) and 3.314 Å (between molecules **B** and **C**), which indicates that trimerization in the stack **1** is rather weak. There is no short inter-molecular metal–ligand contact. Each molecule in the stack **1** shows a planar conformation (Fig. 11(a)). On the other hand, in the stack **2**, inter-planar distances are 3.539 Å (between molecules **D** and **E**) and 3.110 Å (between molecules **E** and **F**), and there are short inter-molecular metal–ligand contacts Ni(**E**)···S(**F**) (3.365(5) Å) and Ni(**F**)···S(**E**) (2.961(5) Å) between molecules **E** and **F**. The molecular conformation is a chair-type for the molecule **E** and a boat-type for the molecule **F** (Fig. 11(b)), while the molecule **D** is almost planar. All these features indicate that the stack **2** is very similar to the stack in the $FeCl_4$ salt. The $FeBr_4$ salt is considered a band insulator, as is the case of the $FeCl_4$ salt.

Other Ni(edo)$_2$ salts. $[Ni(edo)_2]_3(ClO_4)_2$ is a semiconductor ($\rho_{rt}=1.1\times10^4\ \Omega$ cm, $E_a=0.2$ eV) with the monoclinic lattice ($a=16.408(5)$, $b=12.16(1)$, $c=10.818(3)$ Å, $\beta=105.12(6)^\circ$) which suggests that this salt is isostructural with the PF_6 salt. $[Ni(edo)_2]_2GaCl_4$ is an insulator with the triclinic lattice ($a=13.38(2)$, $b=16.15(1)$, $c=7.477(9)$ Å, $\alpha=101.52(8)$, $\beta=101.88(4)$, $\gamma=91.99(7)^\circ$) which suggests that this salt is isostructural with the $FeCl_4$ salt. $[Ni(edo)_2]_2AsF_6$ is a semiconductor ($\rho_{rt}=5.8\times10^2\ \Omega$ cm, $E_a=0.5$ eV) and $[Ni(edo)_2]_3(SbF_6)_2$ is an insulator.

[Ni(ddt)(edo)]$_2$BF$_4$. In contrast to the $Ni(edo)_2$ salts, there is no trimer structure in radical cation salts of the mixed-ligand complexes. The unit cell of $[Ni(ddt)(edo)]_2BF_4$ contains eight donor molecules, two of which are crystallographically independent (molecule **A** and **B** in Fig. 12). In the unit cell, there are two (crystallographically equivalent) donor layers separated by the BF_4 anions. The donor molecules stack along the *b* axis. It is well known that unsymmetrical donor molecules tend to stack alternately, in other words, in the head-to-tail fashion. In this case, however, donor molecules exhibit a head-to-head stacking. Since there is only "glide plane" symmetry, all donor molecules in the crystal align in the same direction. In the stack, inter-planar distances are 3.357 and 3.501 Å, which suggests that the donor molecules are paired to form a dimer. Two modes of overlap (side and top views) are shown in Fig. 13. Both modes are characterized by a twisted overlap with the twist angle between the longitudinal molecular axes of 21°. The short inter-molecular metal–ligand contact is observed only between Ni(**B**) and S(**A**) (3.357(4) Å). Molecules **A** and **B** are almost planar. The terminal ethylene group in the edo ligand of the molecule **B** exhibits a disordered conformation. The most interesting point is that the edo ligands never overlap and the donor molecules overlap only at the ddt site.

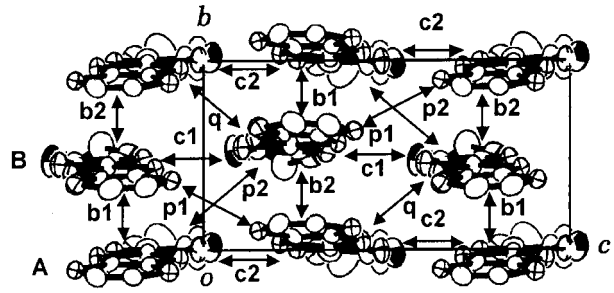

Fig. 12 Donor arrangement in $[Ni(ddt)(edo)]_2BF_4$.

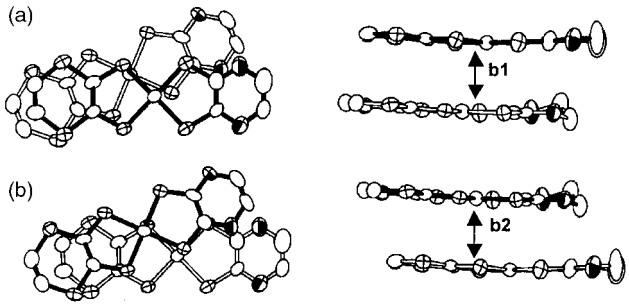

Fig. 13 Modes of overlap in $[Ni(ddt)(edo)]_2BF_4$.

In spite of a promising stoichiometry which could involve a partially occupied band, this compound is a semiconductor with $\rho_{rt}=1.8\times10^2\ \Omega$ cm and $E_a=0.2$ eV. Calculated overlap integrals between HOMOs are listed in Table 4. Tight-binding band calculation suggests that there is no HOMO–LUMO band inversion and the conduction band of this compound is a very narrow HOMO band (Fig. 14). Since this HOMO band is half-filled, it is plausible that the system is in a Mott insulating state.

[Ni(dddt)(edo)]$_3$(FeCl$_4$)$_2$. Fig. 15 shows donor arrangement in the crystal of $[Ni(dddt)(edo)]_3(FeCl_4)_2$. The unit cell contains twelve donor molecules and two (crystallographically equivalent) donor layers. Three crystallographically independent molecules (**A**, **B**, and **C**) are related to molecules **A′**, **B′**, and **C′** by the two-fold axis. Six molecules (**A**, **B**, **C**, **C′**, **B′**, **A′**) are

Table 4 Calculated overlap integrals (*S*) between HOMOs ($\times10^3$) for $[Ni(ddt)(edo)]_2BF_4$ (See Fig. 12)

S	HOMO–HOMO
b1	1.15
b2	−0.25
b3	1.56
c1	−29.57
c2	−7.53
c3	−4.21
c4	−24.95
p1	0.02
p2	1.68
p3	−0.73
q1	−0.7
q2	−0.02

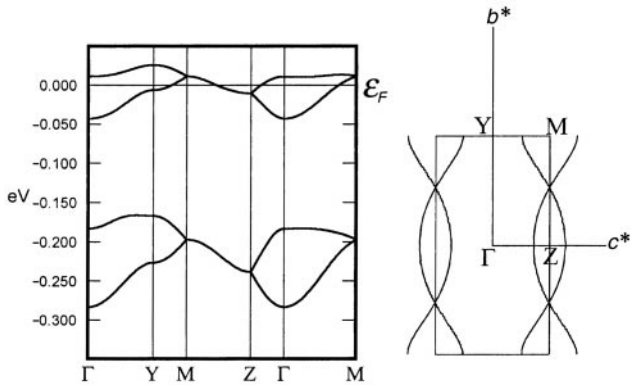

Fig. 14 Calculated band structure and Fermi surface of [Ni(ddt)-(edo)]$_2$BF$_4$.

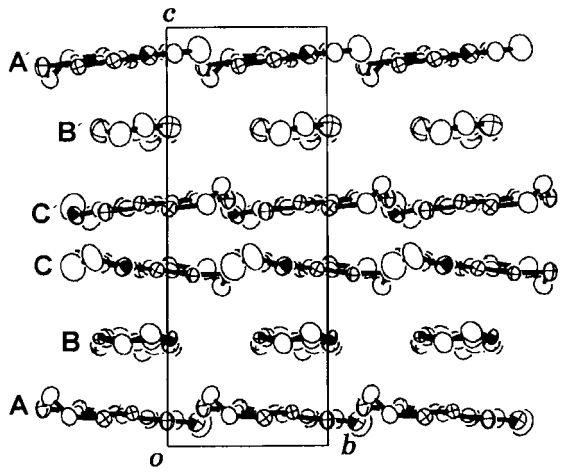

Fig. 15 Donor arrangement in [Ni(dddt)(edo)]$_3$(FeCl$_4$)$_2$.

repeated along the *c* axis. The repeat unit is characterized by three inter-planar distances of 3.226 Å (between molecules **A** and **A′**), 3.535 Å (between molecules **A** and **B**), 3.558 Å (between molecules **B** and **C**), and 3.207 Å (between molecules **C** and **C′**) and two modes of overlap are shown in Fig. 16. In every case, a largely twisted donor arrangement is observed and there is no overlap of the edo ligands. The twist angles between the longitudinal molecular axes are 69° (for **A**···**A′** and **C**···**C′** pairs) and 35° (for **A**···**B**, **B**···**C** pairs). Short inter-molecular metal–ligand contacts Ni(**A**)···S(**A′**) (2.954(2) Å) between molecules **A** and **A′** and Ni(**C**)···S(**C′**) (2.961(5) Å) between molecules **C** and **C′** are observed. The dddt ligand deviates from the molecular plane in the molecules **A** and **C**, while the molecule **B** is almost planar.

As shown in Table 5, calculated overlap integrals between HOMOs indicate that this system has a one-dimensional character along the *c* axis. The stack contains two dimerized pairs (**A**···**A′** and **C**···**C′**). The six-fold structure and the 3 : 2 stoichiometry predict that this system is a semiconductor with an energy gap. Indeed, this salt is a semiconductor with $\rho_{rt} = 1.0 \times 10^4\ \Omega$ cm and $E_a = 0.5$ eV.

[Ni(dtm)(edo)]$_2$ClO$_4$. This salt is a semiconductor with $\rho_{rt} = 1.3 \times 10^4\ \Omega$ cm and $E_a = 0.4$ eV. The unit cell contains sixteen donor molecules and the asymmetric unit contains two crystallographically independent donor molecules (**A** and **B** in Fig. 17). The donor arrangement is characterized by a four-fold stack (···**ABA′B′**···) along the *c* axis. Two modes of overlap are pictured in Fig. 18. The molecule **B** overlaps with the molecule **A** in a head-to-tail fashion with an inter-planar distance of 3.297 Å, and with the molecule **A′** in a head-to-tail fashion with

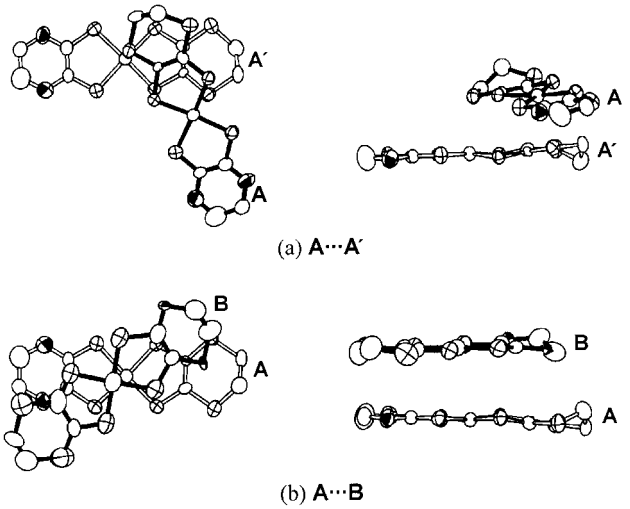

Fig. 16 Modes of overlap in [Ni(dddt)(edo)]$_3$(FeCl$_4$)$_2$.

Table 5 Calculated overlap integrals (*S*) between HOMOs ($\times 10^3$) for [Ni(dddt)(edo)]$_3$(FeCl$_4$)$_2$

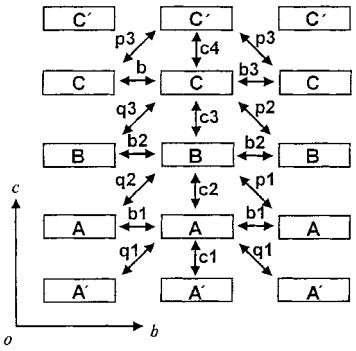

S	HOMO–HOMO
b1	1.15
b2	−0.25
b3	1.56
c1	−29.57
c2	−7.53
c3	−4.21
c4	−24.95
p1	0.02
p2	1.68
p3	−0.73
q1	−0.7
q2	−0.02

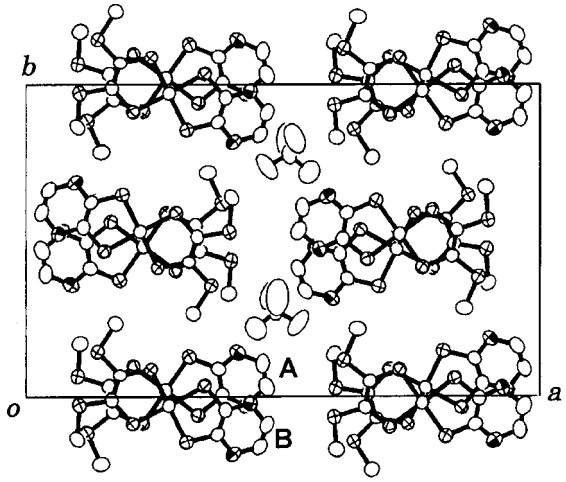

Fig. 17 Crystal structure of [Ni(dtm)(edo)]$_2$ClO$_4$.

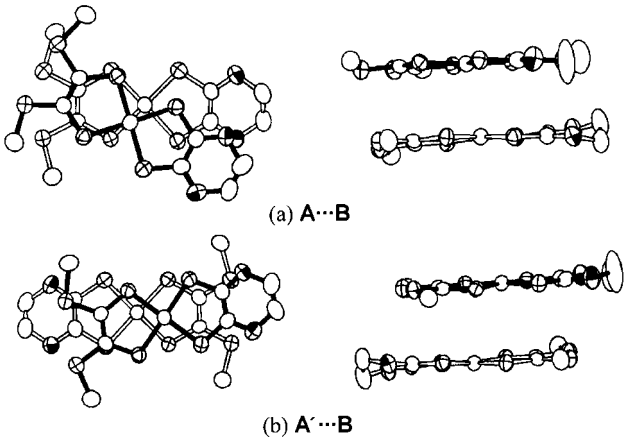

Fig. 18 Modes of overlap in $[Ni(dtm)(edo)]_2ClO_4$.

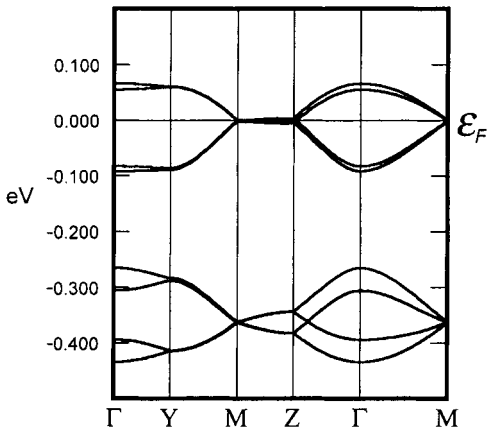

Fig. 19 Calculated band structure of $[Ni(dtm)(edo)]_2ClO_4$. The names of the points in the reciprocal space are the same as those in Fig. 6.

Table 6 Calculated overlap integrals (S) between HOMOs ($\times 10^3$) for $[Ni(dtm)(edo)]_2ClO_4$

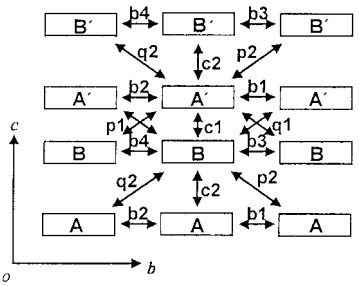

S	HOMO–HOMO
b1	−0.11
b2	−0.16
b3	−0.48
b4	−0.57
c1	−16.72
c2	7.04
p1	0.54
p2	0.009
q1	0.67
q2	−0.06

an inter-planar distance of 3.571 Å. The twist angles between the longitudinal molecular axes are 27° (for the **A**···**B** pair) and 9° (for the **A′**···**B** pair). There is no overlap of the edo ligands, observed for other salts mentioned above. In TTF-based organic conductors, the MeS-group frequently protrudes from the TTF molecular plane. Two MeS-groups in this salt, however, are included in the molecular plane and both **A** and **B** molecules are almost planar.

Calculated overlap integrals among HOMOs listed in Table 6 indicate that this system has a strong one-dimensional character. The donor molecules are dimerized along the c axis, and inter-chain interactions are very weak. The tight-binding band calculation shows that there is not a HOMO–LUMO band inversion and the conduction band is a very narrow and half-filled HOMO band (Fig. 19).

Other salts. $[Ni(ddt)(edo)]_2FeCl_4$ with the monoclinic lattice ($a=33.60(1)$, $b=6.898(3)$, $c=12.787(6)$ Å, $\beta=95.524(8)°$, $V=2949(2)$ Å^3) exhibits rather low resistivity down to low temperature (Fig. 20). $[Ni(dddt)(edo)]_3(PF_6)_2$ has a triclinic lattice with lattice constants of $a=10.59$, $b=31.58$, $c=6.92$ Å, $\alpha=97.10$, $\beta=98.68$, $\gamma=79.31°$. The small size of the crystals prevented conductivity measurement of this salt.

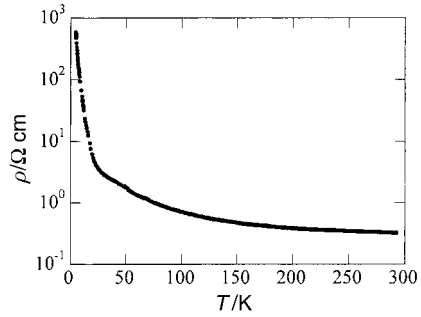

Fig. 20 Temperature dependence of the resistivity for $[Ni(ddt)(edo)]_2FeCl_4$.

Conclusion

The novel donor-type metal–dithiolene complex, $Ni(edo)_2$, and its mixed-ligand derivatives were successfully synthesized. The solubility is largely improved in these complexes and their donor abilities have been confirmed. The radical cation salts based on these newly synthesized metal complexes have exhibited novel donor arrangements including the trimer-based κ-type. It should be noted that the edo ligand shows a repulsive inter-ligand interaction and the face-to-face overlap of the edo ligands seems difficult in the crystal, which frequently leads to the twisted and spanning overlap of the metal complexes. This is in contrast to the BO-based radical cation salts where the organic donor BO shows a strong tendency to aggregate into a two-dimensional layered structure by the aid of both inter-molecular C–H···O and side-by-side heteroatom contacts.[16] In other words, the edo unit seems to have a strong tendency to restrict the mode of overlap, as does the ethylenedioxo unit within BO, but in the opposite way. An origin of this unique feature of the edo ligand remains an open question. We propose to use the characteristics of the edo ligand (improved solubility and unique molecular arrangement) in combination with the extended π-ligands derived from TTF, one of which has been reported to give the single-component neutral compound $Ni(tmdt)_2$ (tmdt = trimethylenetetrathiafulvalenedithiolate) exhibiting metallic conductivity down to 0.6 K.[17] In such a largely elongated π molecule, its poor solubility is a serious problem and the spanning overlap mode plays an important role in the formation of the three-dimensional electronic structure. Further studies are in progress.

Experimental

Synthesis

Ni(edo)$_2$ 3. (Method A) To a stirred solution of 0.83 g (4.7 mmol) of 2,5-dioxa-7,9-dithiabicyclo[4.3.0]non-1(6)-en-8-one **1**[18] and 0.56 g (2.4 mmol) of $NiCl_6{\cdot}6H_2O$ in MeOH (30 mL) was added 0.66 g (4.8 mmol) of K_2CO_3 and 2.51 g (9.5 mmol) of 18-crown-6 in MeOH (35 mL) at room temperature under Ar. After the resultant deep violet solution was stirred for an hour at room temperature, 0.97 g (4.8 mmol) of TCNQ in CH_2Cl_2 (100 mL) was added. The green reaction mixture was stirred for an hour under Ar. The solvent was evaporated under reduced pressure and the residue was column chromatographed using silica gel and CH_2Cl_2 as the eluent. The product was recrystallised from CH_2Cl_2–Pr^iOH (deep blue plates, 0.26 g, 31% yield); Found C, 26.97; H, 2.25; N, 0.00. $C_8H_8O_4S_4Ni$ requires C, 27.06; H, 2.27; N, 0.00%. MS (^{58}Ni, EI): $m/z = 354$ (M^+). (Method B) To a THF solution (50 mL) of 0.35 g (2 mmol) of **1** was added 4.8 mL (4.0 mmol) of 10% Me_4NOH in MeOH at room temperature under Ar. A white precipitate formed immediately and the reaction mixture was stirred for 30 min. The white precipitate was isolated by filtration, washed with THF (3×20 mL), and dissolved in MeOH (10 mL) under Ar. To this solution was added 0.23 g (1.0 mmol) of $NiCl_6{\cdot}6H_2O$ in MeOH (5 mL). After the reaction mixture was stirred for 25 min at room temperature under Ar, 0.42 g (2.1 mmol) of TCNQ in CH_2Cl_2 (50 mL) was added. The reaction mixture was allowed to stir for an hour under Ar. The solvent was evaporated under reduced pressure and the residue was column chromatographed using silica gel and CH_2Cl_2 as the eluent. The product was recrystallised from CH_2Cl_2–Pr^iOH (0.19 g, 54% yield).

Ni(dddt)(edo). A solution of **3** (100 mg, 0.28 mmol) and Ni(dddt)$_2$[19] (123 mg, 0.29 mmol) in 1,2-dichloroethane (50 mL) was refluxed overnight under Ar. The solvent was evaporated under reduced pressure. Column chromatography of the residue using silica gel and CS_2–CH_2Cl_2 (1 : 1) as the eluent afforded the product and recovered **3** (26 mg). The product was recrystallised from CH_2Cl_2–Pr^iOH (dark green powder, 111 mg, 50.9% yield); Found C, 24.85; H, 2.17; N, 0.00. $C_8H_8O_2S_6Ni$ requires C, 24.81; H, 2.08; N, 0.00%. MS (^{58}Ni, EI): $m/z = 386$ (M^+).

Other mixed-ligand complexes were synthesized using the same protocol.

Ni(ddds)(edo). Using 55 mg (0.16 mmol) of **3** and 99 mg (0.16 mmol) of Ni(ddds)$_2$,[20] dark green powder was obtained (11 mg, 7.4% yield); Found C, 20.39; H, 1.60; N, 0.00. $C_8H_8O_2S_4Se_2Ni$ requires C, 19.98; H, 1.68; N, 0.00%. MS (EI): $m/z = 482$ (M^+) with an isotropic pattern of one nickel and two selenium atoms.

Ni(ddt)(edo). Using 67 mg (0.19 mmol) of **3** and 84 mg (0.20 mmol) of Ni(ddt)$_2$,[20] a dark green powder was obtained (35 mg, 24% yield); Found C, 25.04; H, 1.65; N, 0.00. $C_8H_6O_2S_6Ni$ requires C, 24.94; H, 1.57; N, 0.00%. MS (^{58}Ni, EI): $m/z = 384$ (M^+).

Ni(edo)(pdt). Using 32 mg (0.09 mmol) of **3** and 42 mg (0.09 mmol) of Ni(pdt)$_2$,[19] a blue-green powder was obtained (36 mg, 50% yield); Found C, 26.89; H, 2.49; N, 0.00. $C_9H_{10}O_2S_6Ni$ requires C, 26.94; H, 2.51; N, 0.00%. MS (^{58}Ni, EI): $m/z = 400$ (M^+).

Ni(dtm)(edo). Using 59 mg (0.17 mmol) of **3** and 34 mg (0.08 mmol) of Ni(dtm)$_2$,[20] a dark green powder was obtained (41 mg, 66% yield); Found C, 24.84; H, 2.58; N, 0.00. $C_8H_{10}O_2S_6Ni$ requires C, 24.69; H, 2.59; N, 0.00%. MS (^{58}Ni, EI): $m/z = 388$ (M^+).

Electrochemical studies. The cyclic voltammetry experiments were all performed with a YANACO polarographic analyzer P-1100 under Ar at room temperature. A solution of $Bu^n_4NClO_4$ in benzonitrile (0.1 M), Pt working and auxiliary electrodes were used. Potentials were referenced *vs.* Ag/0.01 M $AgNO_3$. The scan rate was 100 mV s^{-1} in every experiment.

Electrochemical crystallization. Single crystals were grown electrochemically in an H-shaped 20 ml cell under an Ar atmosphere at constant current at 20 °C. The donor molecule and a supporting electrolyte were dissolved in chlorobenzene or 1,2-dichloroethane. Detailed conditions are given in the electronic supplementary information.†

X-Ray diffraction data collection and structure determination‡

All data were collected at room temperature using a Weissenberg-type imaging plate (DIP320, MAC Science) or an automatic four-circle diffractometer (MXC18, MAC Science) with graphite-monochromated Mo-Kα ($\lambda = 0.71070$ Å) radiation. $\omega-2\theta$ scans were employed for data collection and Lorentz and polarization corrections were applied in the four-circle diffractometer measurements. The crystal structures were solved by the direct method and refined by the full-matrix least-squares procedure. The refinement was performed using SHELXL-93[21] for Ni(edo)(mnt), [Ni(ddt)-(edo)]$_2BF_4$, [Ni(dddt)(edo)]$_3$(FeCl$_4$)$_2$, and [Ni(dtm)(edo)]$_2ClO_4$, or the teXsan crystallographic software package from Molecular Structure Co. for the others. When the four-circle diffractometer was used, analytical absorption correction was also carried out. In the case of the imaging plate, the absorption correction was included in the scaling process of the image data. The temperature factors were refined anisotropically for the non-hydrogen atoms. All hydrogen atoms were located at calculated positions with fixed isotropic contributions. Crystal data and experimental details are listed in Table 7.‡

Band calculation

The inter-molecular overlap integrals (S) among frontier orbitals were calculated on the basis of the extended Hückel MO method. The semiempirical parameters for Slater-type atomic orbitals are given in Table 8. The band structure and the shape of the Fermi surface were calculated by the tight-binding method, using the transfer integral (t) estimated from the approximation $t = ES$, where E is a constant whose order is of the energy level of the HOMO (−10 eV). The energy gap between HOMO and LUMO (ΔE) was estimated from the molecular orbital calculation of the neutral Ni(edo)$_2$ molecule using density functional theory (DFT) calculations. DFT calculations were performed with Gaussian94[22] using the B3LYP function, and gradient corrections for exchange[23] and correlation[24] effects were introduced. A double-ζ basis with electron core pseudopotential[25] was used.

Electrical resistivity

The measurements of the temperature dependence of resistivity were carried out by the standard four-probe dc method. Gold leads (15 μm diameter) were attached to the sample with carbon paste.

‡CCDC reference number(s) 162731–162739. See http://www.rsc.org/suppdata/jm/b1/b102000p/ for crystallographic files in .cif or other electronic format.

Table 7 Crystal data

Crystal	$Ni(edo)_2$	Ni(dmit)(edo)	Ni(edo)(mnt)	$[Ni(edo)_2]_3\ (PF_6)_2$	$[Ni(edo)_2]_2\ FeCl_4$	$[Ni(edo)_2]_2\ FeBr_4$	$[Ni(ddt)(edo)]_2\ BF_4$	$[Ni(dddt)(edo)]_3\ (FeCl_4)_2$	$[Ni(dtm)(edo)]_2\ ClO_4$
Empirical formula	$NiC_8S_4O_4H_8$	$NiC_7S_7O_2H_4$	$NiC_8S_4O_2N_2H_4$	$Ni_3C_{24}S_{12}O_{12}H_{24}\ P_2F_{12}$	$Ni_2C_{16}S_8O_8H_{16}\ FeCl_4$	$Ni_2C_{16}S_8O_8H_{16}\ FeBr_4$	$Ni_2C_{16}S_{12}O_4H_{12}\ BF_4$	$Ni_3C_{24}S_{18}O_6H_{24}\ Fe_2Cl_8$	$Ni_2C_{16}S_{12}O_8H_{20}Cl$
Formula weight	355.09	403.23	347.07	1355.19	907.84	1085.64	857.19	1556.95	877.90
Crystal system	Triclinic	Monoclinic	Monoclinic	Monoclinic	Triclinic	Monoclinic	Monoclinic	Monoclinic	Orthorhombic
Space group	$P\bar{1}$	Cc	$P2_1/n$	$P2_1/c$	$P\bar{1}$	$P2_1/n$	Cc	$C2$	$Pccn$
a/Å	9.557(6)	11.913(2)	25.420(4)	16.760(1)	13.444(4)	14.989(2)	31.620(5)	34.214(3)	27.211(4)
b/Å	15.26(1)	15.882(3)	7.7460(8)	12.292(1)	16.143(2)	31.944(4)	6.898(1)	7.7180(6)	16.473(3)
c/Å	4.451(5)	8.240(1)	6.0710(8)	10.8640(7)	7.508(1)	14.3620(9)	13.270(2)	23.381(2)	13.801(1)
α /deg	90.29(4)				101.34(1)				
β/deg	97.90(6)	124.06(1)	91.670(7)	104.073(5)	102.42(2)	112.525(7)	92.640(9)	120.889(4)	
γ/deg	86.77(5)				92.10(2)				
V/Å^3	641.9(8)	1291.6(4)	1194.9(3)	2171.0(2)	1555.0(6)	6352(1)	2891.3(8)	5298.4(8)	6186(3)
Z	2	4	4	2	2	8	4	4	8
ρ(calc.)/g cm^{-3}	1.837	2.074	1.929	2.073	1.939	2.270	1.969	1.952	1.885
μ /cm^{-1}	21.58	26.14	23.09	20.46	25.78	72.36	22.21	27.30	21.54
Measured reflections	1738	1647	2693	5592	9062	11751	3044	7003	6089
Independent reflections	748	1087	1713	3371	5782	3854	2198	4642	2458
σ limit	3.0	3.0	3.0	3.0	3.0	3.0	2.0	2.0	2.0
GoF	3.003	3.387	2.583	2.787	2.087	2.779	2.001	1.459	0.776
R, R_w	0.072, 0.069	0.044, 0.046	0.072, 0.182	0.044, 0.043	0.045, 0.049	0.052, 0.049	0.077, 0.153	0.0995, 0.367	0.065, 0.218
Device	IP	IP	IP	IP	4-circle	IP	IP	IP	IP
Refinement on	F	F	F^2	F	F	F	F^2	F^2	F^2

Table 8 The exponents ζ and the ionization energies I_p for atomic orbitals

	Ni			S		O		C		H
	4s	4p	3d	3s	3p	2s	2p	2s	2p	1s
ζ	2.100	2.100		2.122	1.827	2.275	2.275	1.625	1.625	1.000
Double ζ			5.75(0.5798) 2.30(0.5782)							
$-I_p$ (Ryd)	0.805	0.461	1.044	1.620	0.770	2.373	1.087	1.573	0.838	1.000

Acknowledgements

This work was partially supported by the Sumitomo Foundation and a Grant-in-Aid for Scientific Research on Priority Areas (No. 10149103 "Metal-assembled Complexes") from Ministry of Education, Science, Sports and Culture, Japan.

References

1 A. E. Underhill and M. M. Ahmad, *J. Chem. Soc., Chem. Commun.*, 1981, 67; A. Kobayashi, Y. Sasaki, H. Kobayashi, A. E. Underhill and M. M. Ahmad, *J. Chem. Soc., Chem. Commun.*, 1982, 390.

2 E. Canadell, I. E.-I. Rachidi, S. Ravy, J. P. Pouget, L. Brossard and J. P. Legros, *J. Phys. (Paris)*, 1989, **50**, 2967; E. Canadell, S. Ravy, J. P. Pouget and L. Brossard, *Solid State Commun.*, 1990, **75**, 633; H. Tajima, T. Naito, M. Tamura, A. Kobayashi, H. Kuroda, R. Kato, H. Kobayashi, R. A. Clark and A. E. Underhill, *Solid State Commun.*, 1991, **79**, 337.

3 A. Kobayashi and H. Kobayashi, *Handbook of Organic Conductive Molecules and Polymers*, Vol. 1, Ed. H. S. Nalwa, 1997, John Wiley & Sons Ltd., p. 249; P. Cassoux, L. Valade, H. Kobayashi, A. Kobayashi, R. A. Clark and A. E. Underhill, *Coord. Chem. Rev.*, 1991, **110**, 115.

4 R. Kato, Y.-L. Liu, Y. Hosokoshi, S. Aonuma and H. Sawa, *Mol. Cryst. Liq. Cryst.*, 1997, **296**, 217.

5 L. A. Kushch, V. V. Gritsenko, L. I. Buravov, A. G. Khomenko, G. V. Shilov, O. A. Dyachenko, V. A. Merzhanov, E. B. Yagubskii, R. Rousseau and E. Canadell, *J. Mater. Chem.*, 1995, **5**, 1633.

6 T. Suzuki, H. Yamochi, G. Srdanov, K. Hinkelmann and F. Wudl, *J. Am. Chem. Soc.*, 1989, **111**, 3108; M. A. Beno, H. H. Wang, A. M. Kini, K. D. Carlson, U. Geiser, W. K. Kwok, J. E. Thompson, J. M. Williams, J. Ren and M.-H. Whangbo, *Inorg. Chem.*, 1990, **29**, 1599; S. Kahlich, D. Schweitzer, I. Heinen, S. E. Lan, B. Nuber, H. J. Keller, K. Winzer and H. W. Helberg, *Solid State Commun.*, 1991, **80**, 191.

7 G. C. Papavassiliou, A. Terzis and P. Delhaes, *Handbook of Organic Conductive Molecules and Polymers*, Vol. 1, Ed. H. S. Nalwa, 1997, John Wiley & Sons Ltd., p. 151

8 R. Kato, Y. Kashimura, H. Sawa and Y. Okano, *Chem. Lett.*, 1997, 921.

9 D. L. Lichtenberger, R. L. Johnston, K. Hinkelmann, T. Suzuki and F. Wudl, *J. Am. Chem. Soc.*, 1990, **112**, 2302.

10 T. Mori, H. Inokuchi, A. M. Kini and J. M. Williams, *Chem. Lett.*, 1990, 1279.

11 H. Kim, A. Kobayashi, Y. Sasaki, R. Kato and H. Kobayashi, *Bull. Chem. Soc. Jpn.*, 1988, **61**, 579.

12 A. Kobayashi, R. Kato, H. Kobayashi, S. Moriyama, Y. Nishio, K. Kajita and W. Sasaki, *Chem. Lett.*, 1987, 459; H. Urayama, H. Yamochi, G. Saito, K. Nozawa, T. Sugano, M. Kinoshita, S. Sato, K. Oshima, A. Kawamoto and J. Tanaka, *Chem. Lett.*, 1988, 55; A. Kini, U. Geiser, H. H. Wang, K. D. Carlson, J. M. Williams, W. K. Kwok, K. G. Vandervoort, J. E. Thompson, D. L. Stupka, D. Jung and M.-H. Whangbo, *Inorg. Chem.*, 1990, **29**, 2555.

13 R. Kato, H. Kobayashi, H. Kim, A. Kobayashi, Y. Sasaki, T. Mori and H. Inokuchi, *Chem. Lett.*, 1988, 865.

14 E. B. Yagubskii, A. I. Kotov, E. E. Laukhina, A. A. Ignatiev, L. I. Buravov and A. G. Khomenko, *Synth. Met.*, 1991, **41–43**, 2515.

15 H. Inokuchi, G. Saito, P. Wu, K. Seki, T. B. Tang, T. Mori, K. Imaeda, T. Enoki, Y. Higuchi, K. Inaka and N. Yasuoka, *Chem. Lett.*, 1986, 1263.

16 S. Horiuchi, H. Yamochi, G. Saito, K. Sakaguchi and M. Kusunoki, *J. Am. Chem. Soc.*, 1996, **118**, 8604.

17 H. Tanaka, Y. Okano, H. Kobayashi, W. Suzuki and A. Kobayashi, *Science*, 2001, **291**, 285.

18 K. Hartke and T. Lindenblatt, *Synthesis*, 1990, 281.

19 R. Kato, H. Kobayashi, A. Kobayashi and Y. Sasaki, *Bull. Chem. Soc. Jpn.*, 1986, **59**, 627.

20 The neutral complexes $[Ni(L)_2]^0$ (L = ddds, ddt, and dtm) were synthesized by the similar procedure reported in ref. 19.

21 G. M. Sheldrick, SHELXL-93, Program for the Refinement of Crystal Structures. University of Göttingen, Germany, 1993.

22 M. J. Frisch, G. W. Trucks, H. B. Schlegel, P. M. Gill, B. G. Johnson, M. A. Robb, J. R. Cheeseman, T. Keith, G. A. Petersson, J. A. Montgomery, K. Raghavachari, M. A. Al-Laham, V. G. Zakrzewski, J. V. Oritz, J. B. Foresman, J. Cioslowski, B. B. Stefanov, A Nanayakkara, M. Challacombe, C. Y. Peng, P. Y. Ayala, W. Chen, M. W. Wong, J. L. Andres, E. S. Replogle, R. Gomperts, R. L. Martin, D. J. Fox, J. S. Binkley, D. J. Defrees, J. Baker, J. P. Stewart, M. Head-Gordon, C. Gonzalez and J. A. Pople, Gaussian94, Revision E.2, Gaussian Inc., Pittsburgh, PA, 1995.

23 A. D. Becke, *Phys. Rev. A*, 1988, **38**, 3098.

24 C. Lee, W. Yang and R. G. Parr, *Phys. Rev. B*, 1988, **38**, 372.

25 P. J. Hay and W. R. Wadt, *J. Chem. Phys.*, 1985, **82**, 270; W. R. Wadt and P. J. Hay, *J. Chem. Phys.*, 1985, **82**, 284; P. J. Hay and W. R. Wadt, *J. Chem. Phys.*, 1985, **82**, 299.